 doi:10.20944/preprints202208.0228.v1

Article

Calculating the Speed Ratio of Wind Turbines with General Cone and Axis Angle for the Unsteady Blade Element Momentum Theory (UBEMT)

Dieter Scholz [1,*]

[1] Aircraft Design and Systems Group (AERO), Hamburg University of Applied Sciences
* Correspondence: info@ProfScholz.de

Abstract: Purpose – Extend the Blade Element Momentum Theory (BEMT) such that rotors with pronounced cone and axis angle (tilt or yaw) can be calculated. Derive an equation for the speed ratio (lambda) as a function of Tip Speed Ratio (TSR), radius, blade, cone and axis angle. This converts the BEMT into an Unsteady BEMT or UBEMT. Present the Wagner rotor as one such rotor geometry. --- Methodology – Literature review and calculations. --- Findings – The UBEMT can be used to calculate highly unconventional rotor geometries. --- Research Limitations – Although the aerodynamic coefficients used in the UBEMT are from measurements in steady flow conditions, they can be used with success. --- Practical Implications – Also conventional Horizontal Axis Wind Turbines (HAWT) with noticeable cone and axis angle should be calculated with the UBEMT. The accuracy of power calculations of these HAWTs can be slightly improved. --- Originality – Analytic equations for rotors with cone and axis angle have barely been discussed.

Keywords: Wind power; Wind turbines; Aerodynamics; Differential Geometry; Airfoils; Blade Element Momentum Theory; BEMT; BEM; HAWT; Wagner rotor

1. Introduction

For the past decades, wind power is the leading source of renewable energy. It is the world's fastest growing energy source due to its reliability and cost-effectiveness [1]. Wind energy systems [2] or **wind turbines** [3,4] are well covered in textbooks in English or other languages like German [5-8].

The dominant wind turbine design is the **Horizontal Axis Wind Turbine** (HAWT) with blades usually rotating in front of the tower. A closer look reveals that HAWTs often have an axis with a small angle to the horizon. Furthermore, the blades may show an angle with the axis not exactly 90° (Figure 1). Such angles are used to ensure clearance between the blades and the tower, considering rotor blade bending under loads. Clearance to the tower is not only common sense, but also required by the international standard IEC 61400-1 [10]. **Cone angle**, **axis angle** and overhang (Figure 2) may be used concurrently, but can only be used to a limited extent. Tilting beyond 5° may introduce unwanted cyclic loads, while coning results in a moment at the blade root due to centrifugal forces on the blade [1]. Coning and tilting also results in a reduction of power or require longer blades to maintain power [12]. An additional overhang causes increased loads on rotor bearings.

Installing **wind energy systems offshore** has several advantages. Additional sites become available, wind speeds are higher than on land, and turbulence is lower. The visual impact is reduced and noise impact on humans is also reduced. Certainly, there are also many disadvantages with offshore wind energy. Disadvantages combined result in higher costs. For water depths up to 50 m, wind turbines are installed on the sea floor. At a certain water depth, floating structures are less expensive than those installed on the

Preprints (www.preprints.org) | NOT PEER-REVIEWED | Posted: 12 August 2022 doi:10.20944/preprints202208.0228.v1

sea floor [1]. Figure 3a shows one example of a floating HAWT. A long cylindrical buoy is anchored with mooring lines. It floats upright due to ballast at its base.

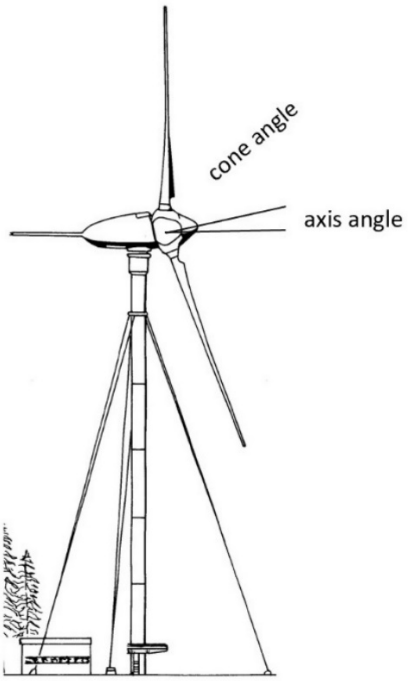

Figure 1. Axis angle (nominal: 10°, oscillating nave) and cone angle (9°) of the German 3 MW research wind turbine GROWIAN ("Große Windenergieanlage" – "large wind turbine"), 1983 – 1987. The blades rotated on the leeward side of the tower. Based on [9].

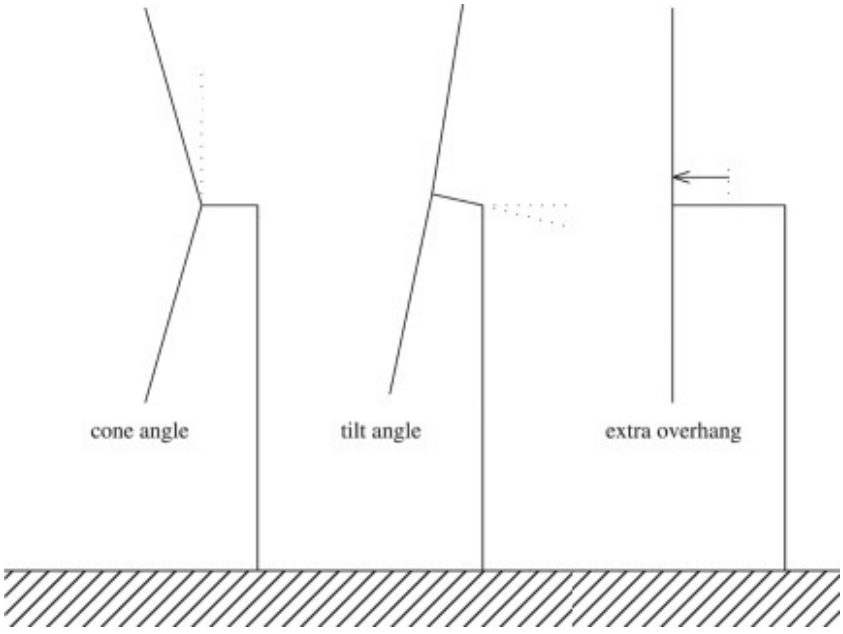

Figure 2. Geometry variations with cone angle and axis (tilt) angle of a HAWT to ensure clearance between blade and tower. Based on [11].

The **Wagner rotor** (Figure 3b) is a proposal from the 1980th especially as a wind turbine for deep water offshore use. The idea is to mount a wind turbine without a tower on a conventional ship. The Wagner rotor applies large cone and axis angles (Figure 4).

Preprints (www.preprints.org) | NOT PEER-REVIEWED | Posted: 12 August 2022 doi:10.20944/preprints202208.0228.v1

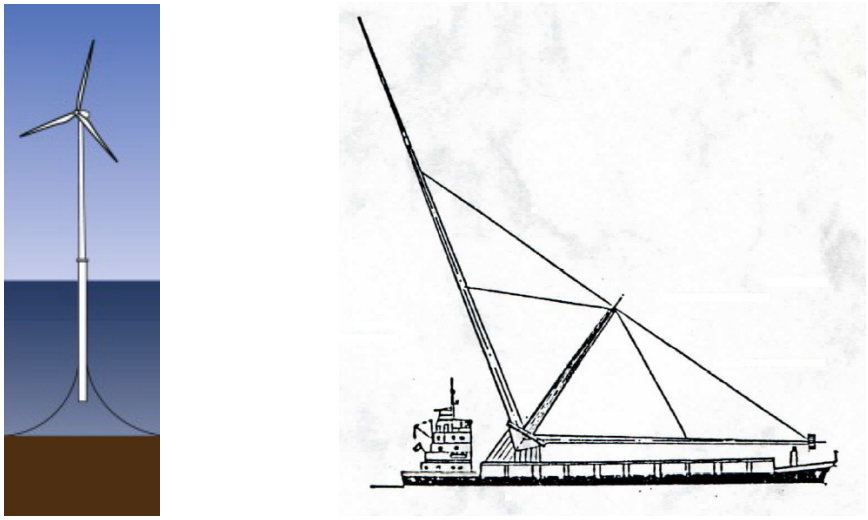

(a) (b)

Figure 3. Deep water offshore wing turbines. (**a**) Wind turbine with horizontal axis mounted on a perpendicularly floating buoy (based on [1]). (**b**) Asymmetric Wagner rotor with pronounced cone and axis angle mounted on a ship (reproduced from [12]).

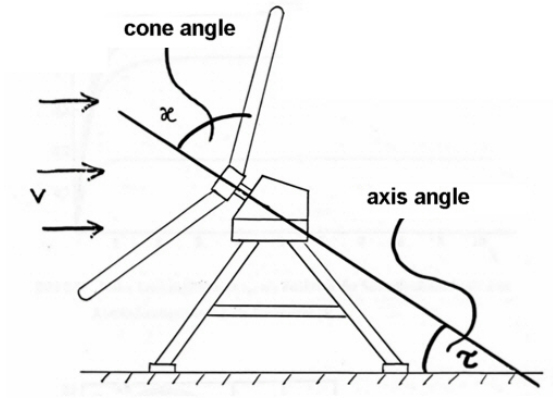

Figure 4. Wagner rotor onshore. Defined are cone angle, κ (kappa) and axis angle, τ (tau). The axis angle leads to tilt of the rotor plane. Based on [12].

Calculating the **power output of wind turbines with pronounced cone and axis angle** as shown on Figure 1, Figure 3b, and Figure 4 has to take this geometry into account. Lift and drag on the blades depend on the relative speed. Blades on a tilted (more horizontal) rotor disc move against the wind during one half of the revolution and move with the wind during the other half of the revolution. The same is true if the rotor would experience a yaw angle instead. With a cone angle it has to be noted that only the component of the relative wind vector shows an effect that acts on the airfoil. A flow along the length of the blade remains without primary effect.

Wind power calculations are based on a nondimensional rotational speed known as the **tip speed ratio** (TSR). For TSR, the Greek letter λ (lambda) is used in equations. To be more precise, λ can be calculated anywhere along the length of the blade at a radius r. TSR is calculated at the blade tip, where $r = R$ and $\lambda = \lambda_t$. The index t stands for "tip". For HAWT, the speed ratio, $\lambda(r)$ is the ratio of circumferential speed, u and wind speed, v. ω (omega) is the angular velocity in 1/rad and ν (nu) is the rotational speed in 1/s or in revolutions per minute (rpm) divided by 60.

$$\lambda(r) = \frac{u(r)}{v} = \frac{\omega\, r}{v} = \frac{2\pi\, v\, r}{v} \quad ; \quad \lambda_t = \frac{\omega\, R}{v} = \frac{2\pi\, v\, R}{v} \tag{1}$$

 doi:10.20944/preprints202208.0228.v1

This article shows, how cone and axis angle can be considered in the calculation of power output of wind turbines and how this can be done based on an extended calculation of λ. The practical purpose of this article is to add an equation $\lambda = \lambda\ (r,\tau,\kappa,\theta)$ to the aerodynamic calculation of wind turbines and to extend the Blade Element Momentum Theory (BEMT) to certain unsteady flow conditions. The equation $\lambda = \lambda\ (r,\tau,\kappa,\theta)$, which is based on radius, cone and axis angle is not new. It had been derived in the Appendix of a report, written by the author in 1985 [12]. This German report was made available online decades later and published in repositories. However, the equation never reached any larger visibility.

A **literature review** including above mentioned sources [1-10] and more, e. g. [13-18] showed no mention of including cone and axis angle into the calculation of power output of wind turbines. In one paper [19] the cone angle was systematically varied, leaving the axis angle always at 0°. The authors found that the turbine suffers a reduction of power with a cone angle, κ less than 90°. Calculations were done with Qblade from the Technical University in Berlin, Germany. The more recent version of Qblad [20] has moved from the BEMT to the Lifting Line Free Vortex Wake (LLFVW) method. The numeric code allows input of rotor cone angle, rotorshaft tilt angle, and/or rotor yaw angle on the fist tab of the simulation setup dialog. Qblade allows superb visualization of the rotor wake in addition to the output of rotor (global) parameters like turbine power. The inclusion of yaw in the BEMT (without cone angle) is covered in [21].

Structure of the article: Chapter 2 introduces a wind turbine with pronounced cone and axis angle. Chapter 3 talks about fundamentals of the Blade Element Momentum Theory (BEMT). Chapter 4 extends the BEMT to the unsteady case due to pronounced cone and axis angle. Chapter 5 derives $\lambda = \lambda\ (r,\tau,\kappa,\theta)$ as input to the Unsteady Blade Element Momentum Theory (UBEMT). Other documents written or supervised by the author, include on the same topic:

- Results from the UBEMT applied to the Wagner rotor [12].
- Equations for the BEMT, systematically listed and derived [22, 24].
- The BEMT applied to a HAWT compared to measurements [23].
- The setup of an Excel program for the UBEMT and its application [24].

As such, these results are not repeated here in detail.

2. The Wagner Rotor

The Wagern rotor (Figure 5) is named after his inventor Dr. G. Wagner from Sylt, Germany. He published his idea in the early 1980th. Here are the abstracts with his own words.

Abstract from 1982 in [25]:

A newly developed wind turbine is described. Its rotor - called Wagner rotor after its inventor - is neither based on a horizontal nor a vertical shaft. The shaft has an inclination angle of 50°. The turbine has anchored a rotor blade following the principle of a suspension bridge … The whole plant is mounted on a ship.

Abstract from 1982 in [26]:

During the past year, a large model of a floating windmill has been working near Sylt, the most northerly Island off Germany. Its maximum power is 250 kW, the length of the blade is 25 m and the length of the ship, 30 m … The advantages of offshore windmills are their low price (500 U.S.$/kW), short building time and lack of problems with transportation or siting … Floating windmills have several special problems. First there is the necessity of a low centre of gravity, secondly the construction must be simple and robust. The Wagner rotor was developed with consideration of these problems. The axis of the Wagner rotor has a tilt angle of 45° or 55°; the angles between blades and axis (cone angle) are 55°. The bearings, gears, generator and nacelle are inside the ship. The tips of the blades are also connected with wire ropes to a pylon positioned on the axis. The disadvantage of the Wagner rotor is that the blades are 1.7 times longer than the wings of horizontal axis turbines with equal power rating. However, the cost of the blades is 10% of the total cost of the windmill (including the ship), and therefore this is of no particular concern.

Preprints (www.preprints.org) | NOT PEER-REVIEWED | Posted: 12 August 2022 doi:10.20944/preprints202208.0228.v1

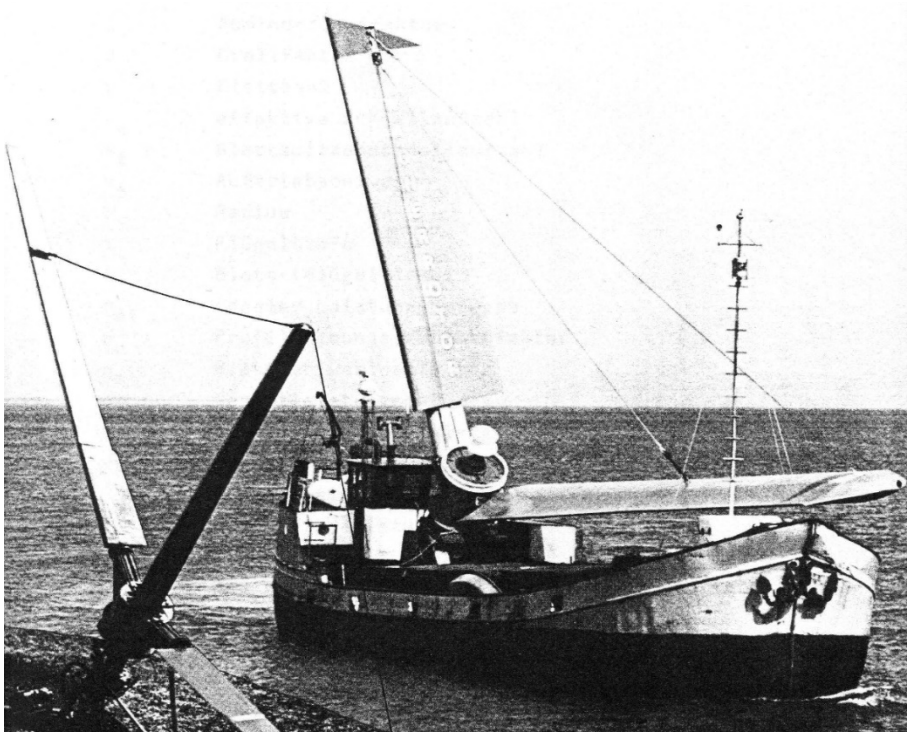

Figure 5. Two Wagner rotors. Left: An onshore version. Right: A deep water offshore version. [12]

In 1985 test results from Germanischer Lloyd, Hamburg, Germany, financed by the German Ministry for Research and Technology were published in [27]:
For utilization of wind energy at sea Dr. Wagner from List/Sylt has proposed a novel system, a prototype of which he installed aboard the vessel Tanja I. The operating performance of the prototype Wagner Rotor I was to be determined. The investigation programme was not confined to determination of wind velocity and direction and of the output capable of being picked up at the generator. Beyond this, it was to be attempted to simultaneously determine the stresses acting on the rotor blade and structures adjacent to the foundation. Also, the vessel's vibration behaviour and stability during operation of the system was to be assessed. The system presented did not permit any performance/wind velocity charts to be prepared, as it was impracticable to operate the system in the stationary condition for a prolonged period and as the system was not provided with a governing device. The Wagner Rotor I has to be started by means of a motor and only with wind velocities in excess of 10 m/sec it continued to rotate automatically. Related to the size of the installation its mechanical and electrical output measured is extremely low. Considering the limited quantity of energy generated per year it appears to be impossible to derive any substantial economic benefit from the system in the concept presented.

Despite this devastating result, it may still be worth to look again at the old concept for deep water offshore application. It needs to be considered that the ship-mounted wind turbine of Figure 5 was based on a one-man-effort and his private finances. The Wagner rotor has certainly the potential to produce power. The power reduction factor compared to the HAWT can be calculated.

A first order calculation looks at the rotor disc geometry. Following a first intuitive idea, a cone angel $\kappa = 45°$ could be applied on a ship (Figure 6). To have the rotor blade in its lowest position horizontally along the deck of the ship, the axis angle would need to be $\tau = \kappa = 45°$. From a rotor blade length, L follows a Radius, $R = L \sin \kappa$, which forms the semi-major axis, a of the ellipse. The length of the semi-minor axis, b of the ellipse is calculated from $b = R \cos \tau = L \sin \kappa \cdot \cos \kappa$.

Preprints (www.preprints.org) | NOT PEER-REVIEWED | Posted: 12 August 2022 doi:10.20944/preprints202208.0228.v1

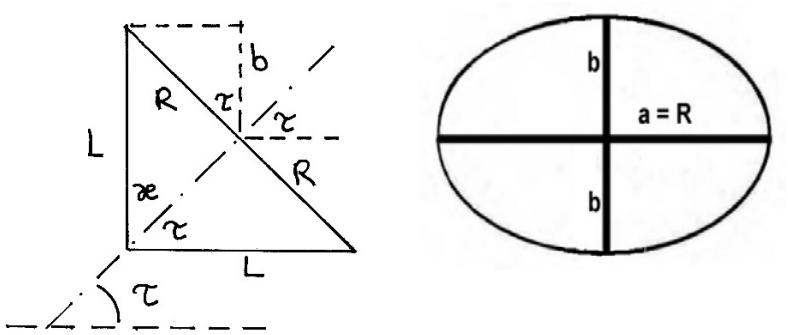

(a) **(b)**

Figure 6. Geometry of the Wagner rotor. (**a**) Side view of the Wagner rotor shown with a cone angle of 90°. L is the length of the rotor blade. Angles are defined as in Figure 4. (**b**) The projected area towards the wind is an ellipse with semi-major axis, $a = R$ and semi-minor axis, b.

The projected area of the Wagner rotor is an ellipse with area, A_{WR}. The horizontal axis wind turbine has a projected area, A_{HAWT}. This is the largest possible area swept by a rotor blade of length L. The Wagner rotor should maximize the ratio of the two projected areas. Equation (6) is plotted as Figure 7.

$$A_{WR} = \pi\, a\, b = \pi\, L \sin\kappa \cdot L \sin\kappa \cdot \cos\kappa \tag{2}$$

$$\text{with } \sin x \cos x = \frac{1}{2}\sin 2x \tag{3}$$

$$A_{WR} = \frac{1}{2}\pi L^2 \cdot \sin\kappa \cdot \sin 2\kappa \tag{4}$$

$$A_{HAWT} = \pi\, L^2\,; \tag{5}$$

$$\frac{A_{WR}}{A_{HAWT}} = \frac{1}{2} \cdot \sin\kappa \cdot \sin 2\kappa \tag{6}$$

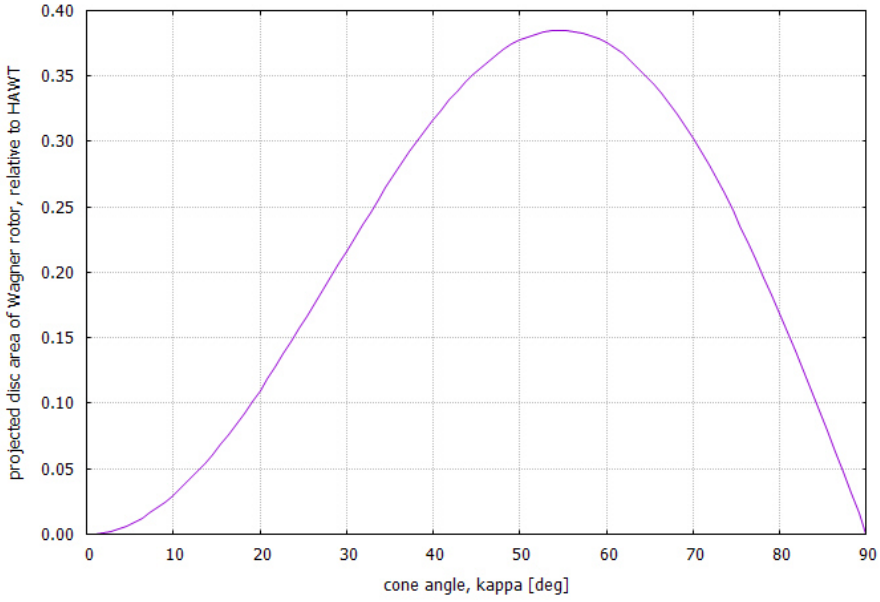

Figure 7. The projected disc area of the Wagner rotor, A_{WR} relative to the maximum possible disc area as given by the horizontal axis wind turbine, A_{HAWT}. Plot of (6). Maximum at $\kappa = 54.74°$ with $A_{WR} / A_{HAWT} = 0.3849$.

Preprints (www.preprints.org) | NOT PEER-REVIEWED | Posted: 12 August 2022 doi:10.20944/preprints202208.0228.v1

The maximum of the ratio of the two projected areas can be found from the derivative of (6) set to zero. This yields an optimum cone angle, $\kappa = 54.74° \approx 55°$. Wagner also proposes this number in [26], which is more than the first intuitive idea of a cone angel, $\kappa = 45°$ (Figure 6a). A cone angel $\kappa = 55°$ is depicted in Figure 3b. With $\kappa = 55°$, (6) yields a ratio of 0.3849. With a rotor blade longer by a geometry factor of 1.61 the same projected area could be achieved as with the HAWT. Conservatively rounded up, this is the factor 1.7, which Wagner mentions in [26].

Calculations in [12] show that the overall aerodynamic efficiency of the Wager rotor is only about half of the efficiency of a HAWT. To make up also for this, the projected area would need to be twice as big and the rotor blade longer by a factor of $\sqrt{2}$. Together with the geometry factor, the rotor blades of a geometrically optimum Wagner rotor would need to be longer by a factor of $1.61 \cdot \sqrt{2} = 2.28$. With the same rotor blade as used for a HAWT, the Wagner rotor only produces $0.385 \cdot ½$ or 19% of the HAWT output.

The Wagner rotor using the same rotor blade would only be economically superior to a floating deep water HAWT, if overall operating costs are more than five times lower.

3. The Blade Element Momentum Theory (BEMT)

Almost all engineering-level aerodynamic design calculations for Horizontal Axis Wind Turbines (HAWT) are done with the Blade Element Momentum Theory (BEMT) [28]. Since the flow changes with the radius of the rotor, the rotor disc is divided into several annular rings at radius, r (Figure 8). The aerodynamic forces at each blade element are represented by the lift coefficient and drag coefficient known for the airfoil in place. At best, aerodynamic coefficients should be available from wind tunnel measurements for all 360° of angle of attack. Conservation of energy tells us that the wind turbine reduces the velocity of the flow when power is extracted. Conservation of angular momentum tells us that the braking momentum of the generator must be equal to the angular momentum exerted on the flow. This starts the flow to rotate. The energy of the rotating flow is dissipated downstream and lost.

The angle of attack at the airfoil follows from the angular velocity of the blade and the wind speed. Of interest is the flow at the disc. It is assumed that half of the wind speed reduction and half of the final rotational speed is present in the plane of the rotor disc. At the disc the speed ratio is called **effective speed ratio**, $\lambda_2 = u_2 / v_2$, where the "2" denotes the flow condition at the rotor disk. From λ_2 the angle of attack at the airfoil can be calculated. The calculation is iterative. Vortices are shed from the tip of the blades and are accounted for by a tip loss factor. Equations are given in [12, 22-24].

If only the change of energy and axial momentum is considered (which is equivalent to an operation with infinitely high rotational speed), optimum power extraction is found with a final reduction of the horizontal speed to 1/3 of wind speed. The horizontal speed cannot be reduced to zero, because the air needs to flow continuously past the turbine. With the reduction of the horizontal speed to 1/3 of its original value, a maximum of $C_P = 16/27$ or 59% of the power of the moving air can be extracted. At lower rotational speed (or speed ratio, λ) the power coefficient, C_P reduces drastically. The power extracted from the rotor is

$$P = C_P \frac{1}{2} \rho A v^3 \quad . \tag{7}$$

A is the (projected) disc area, ρ is the air density, and v is the wind velocity. C_P is the result of the BEMT. An example for a C_P-λ-diagram is given in Figure 9.

Preprints (www.preprints.org) | NOT PEER-REVIEWED | Posted: 12 August 2022 doi:10.20944/preprints202208.0228.v1

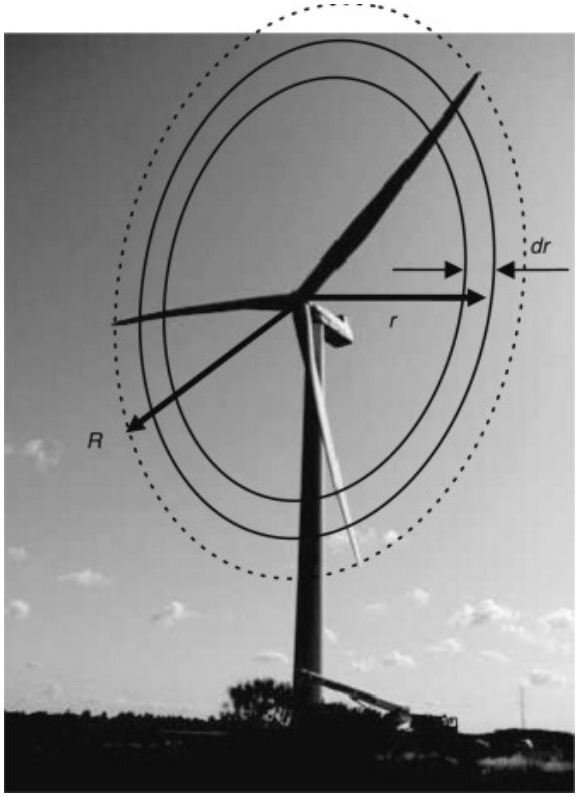

Figure 8. The Blade Element Momentum Theroy (BEMT) divides the disc area into several annular rings of width *dr* at a representative radius, *r* [2].

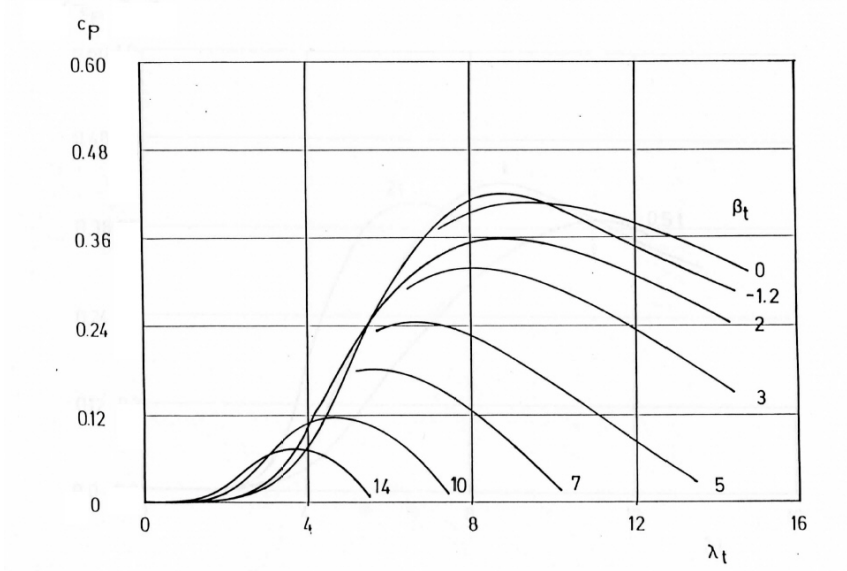

Figure 9. Example of a C_P-λ-diagram. Plotted is the power coefficient, C_P versus tip speed ratio λ_t with blade tip angle, β_t as parameter. Wind energy converter "Adler 25" of Maschinenfabrik Köster, Heide, Germany. Calculations with (U)BEMT [23].

Most wind energy textbooks touch upon the BEMT, but often do not go to the root of the equations with required iteration. This article has to refer to previous work. For historical reasons, there are different ways of writing the equations of the BEMT. As such, it can be confusing when working with different sources.

Preprints (www.preprints.org) | NOT PEER-REVIEWED | Posted: 12 August 2022 doi:10.20944/preprints202208.0228.v1

4. The Unsteady Blade Element Momentum Theory (UBEMT)

Unsteady flow at the blade element can be caused by turbulence or by changing wind speeds with height [22]. This is not the topic here. But even in uniform flow, unsteady flow at the blade can be caused by an axis angle or a yaw angle. A cone angle by itself does not cause unsteady flow, but further complicates the calculation.

As explained in the Introduction, blades on a tilted rotor disc move against the wind during one half of the revolution and move with the wind during the other half of the revolution. In order to account for these changes with blade angle, blade elements are not only differentiated by radius, r (Figure 8), but in addition also by blade angle, θ (Figure 10).

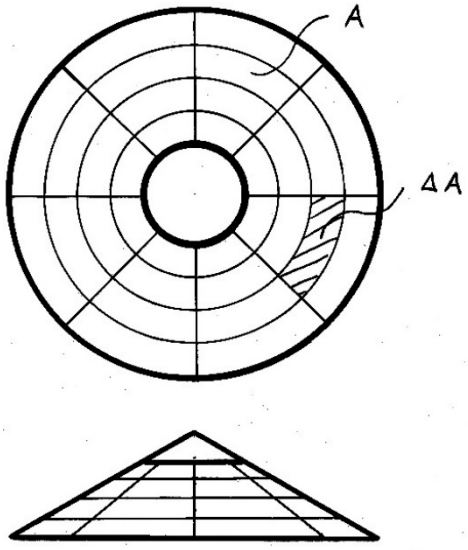

Figure 10. Blade elements of the Unsteady Blade Element Momentum Theroy (UBEMT), which is considering cone and axis angle. The total area, A is divided into many elements ΔA along the radius, r and the blade angle, θ.

In the same way as in the BEMT, the angle of attack can be calculated for each blade element from the effective speed ratio at the location of the disc, λ_2. The Unsteady Blade Element Momentum Theory (UBEMT) adds to the BEMT another calculation loop to account for the blade angle, θ (Figure 11) and adds an equation for the speed ratio, λ, which is derived in the next chapter. In [23] it was found that a HAWT with an axis angle of 10° showed not more than 1% reduction in the power coefficient when the UBEMT was used instead of the assumption of a truly horizontal axis. This is a reassurance than can only be obtained from a calculation with the UBEMT.

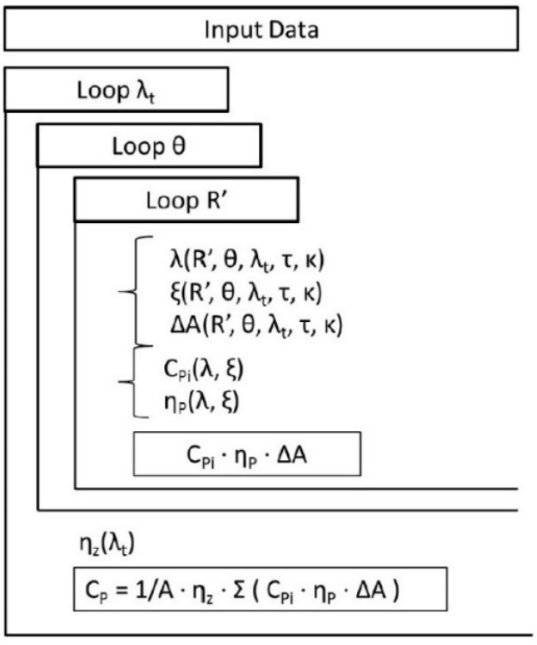

Figure 11. Unsteady Blade Element Momentum Theory (UBEMT). A C_P-λ-Diagram is calculated in three nested loops. Details in [12].

Preprints (www.preprints.org) | NOT PEER-REVIEWED | Posted: 12 August 2022 doi:10.20944/preprints202208.0228.v1

5. Derivation of the Speed Ratio λ for a Wind Turbine with Cone and Axis Angle

The wind speed is written as a vector $\overrightarrow{v_w}$. The calculation requires the wind to flow only from the inside to the outside of the cone surface. This requirement is fulfilled (Figure 12) if:

$$\tau < \kappa \tag{8}$$

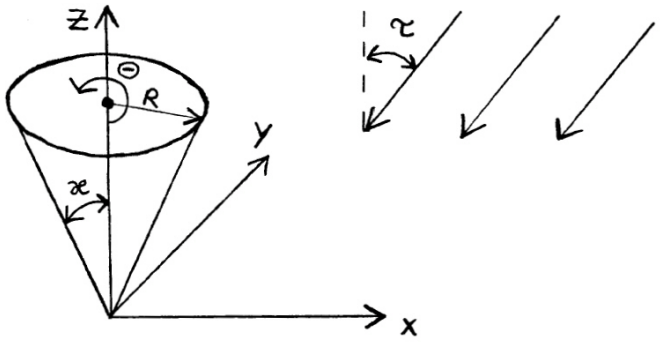

Figure 11. Chosen Cartesian coordinates to derive the speed ratio for a wind turbine with cone and axis angle [12]. The turbine rotates about the z-axis. The wind vector (or the turbine) is tilted by an angle τ with respect to the z-axis in the x-z-plane. Tilt, τ can also represent yaw.

The calculation of the speed ratio, λ is divided into three parts:
Calculation of the velocity v.
Calculation of the velocity u.
Calculation of λ from $\lambda = u/v$.

5.1 Calculation of the Velocity v Perpendicular to the Surface

Differential geometry is used to calculate the component of $\overrightarrow{v_w}$ perpendicular to the cone surface. All data is given in Cartesian coordinates. The cone surface is described by:

$$\vec{x} = (r\cos\theta,\ r\sin\theta,\ r\cot\kappa) \tag{9}$$

with $0 \le r \le R$ and $0 \le \theta \le 2\pi$.

R is the biggest possible radius in the cone (Figure 6). The Wind speed is described by

$$\overrightarrow{v_w} = (-v_w\sin\tau,\ 0,\ -v_w\cos\tau) \tag{10}$$

$\overrightarrow{x_r}$ is the partial derivative of the vector $\vec{x}$ with respect to r.
$\overrightarrow{x_r} = (x_r,\ y_r,\ z_r)$ is the tangent on the cone shell in r-direction.

$\overrightarrow{x_\theta}$ is the partial derivative of the vector $\vec{x}$ with respect to θ.
$\overrightarrow{x_\theta} = (x_\theta,\ y_\theta,\ z_\theta)$ is the tangent on the cone shell in θ-direction.

$$\vec{n} = \overrightarrow{x_r} \times \overrightarrow{x_\theta} \tag{11}$$

The normal vector $\vec{n}$ is perpendicular to the cone shell surface described by of $\overrightarrow{x_r}$ and $\overrightarrow{x_\theta}$ in point $\vec{x}$. The normal vector results from the vector product of $\overrightarrow{x_r}$ and $\overrightarrow{x_\theta}$.

$$\vec{n} = \begin{pmatrix}\cos\theta\\ \sin\theta\\ \cot\kappa\end{pmatrix} \times \begin{pmatrix}-r\sin\theta\\ r\cos\theta\\ 0\end{pmatrix} = r\begin{pmatrix}-\cot\kappa\cos\theta\\ -\cot\kappa\sin\theta\\ 1\end{pmatrix} \tag{11}$$

Preprints (www.preprints.org) | NOT PEER-REVIEWED | Posted: 12 August 2022 doi:10.20944/preprints202208.0228.v1

The projection of $\overrightarrow{v_w}$ in direction $-\vec{n}$ is

$$v_{w\,\vec{n}} = \frac{-\overrightarrow{v_w}\,\vec{n}}{|\vec{n}|} \tag{12}$$

$-\overrightarrow{v_w}\,\vec{n}$ is a scalar product. The negative direction must be selected for the normal vector because $\vec{n}$ is directed inward into the cone.

$$-\overrightarrow{v_w}\,\vec{n} = \begin{pmatrix} -v_w \sin\tau \\ 0 \\ -v_w \cos\tau \end{pmatrix} \cdot r \begin{pmatrix} -\cot\kappa \cos\theta \\ -\cot\kappa \sin\theta \\ 1 \end{pmatrix} = r\, v_w\, (\cos\tau - \sin\tau\ \cot\kappa \cos\theta)$$

The length of the vector its

$$|\vec{n}| = r\sqrt{(-\cot\kappa\cos\theta)^2 + (-\cot\kappa\sin\theta)^2 + 1^2}$$

$$|\vec{n}| = r\sqrt{\cot^2\kappa + 1} \quad .$$

$$v = v_{w\,\vec{n}} = \frac{-\overrightarrow{v_w}\,\vec{n}}{|\vec{n}|} = v_w\, \frac{(\cos\tau - \sin\tau\cot\kappa\cos\theta)}{\sqrt{\cot^2\kappa + 1}} \tag{12}$$

The projected velocity $v_{w\,\vec{n}}$ perpendicular to the cone's surface is the required velocity v.

5.2 Calculation of the Tangential Velocity u

The circumferential or tangential velocity u also depends on the wind speed. It increases when the wing runs against the wind and vice versa.

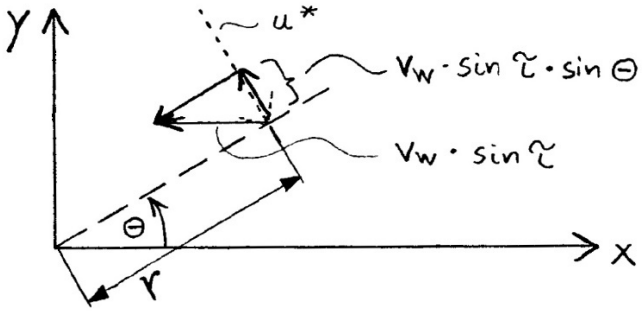

Figure 12. Velocities on the rotating blade [12].

$$u^* = \dot{\theta} r = \omega r \tag{13}$$

$$u = \omega r - v_w \sin\tau \sin\theta \tag{14}$$

5.3 Calculation of the Speed Ratio λ

From the calculated speeds u and v, the speed ratio λ can now be calculated.

$$\lambda = \frac{u}{v} = \frac{(\omega r - v_w \sin\tau \sin\theta)\sqrt{\cot^2\kappa + 1}}{v_w\,(\cos\tau - \sin\tau \cot\kappa \cos\theta)} \tag{15}$$

The tip-speed ratio (TSR) at the blade tip on the Wagner rotor is conveniently defined as

$$\lambda_t = \frac{u}{v} = \frac{\omega R}{v_W} \quad . \tag{16}$$

Solved for ω

$$\omega = \frac{\lambda_t v_W}{R} \tag{16}$$

and introduced into (15) yields the final equation

$$\lambda = \frac{\left(\lambda_t \frac{r}{R} - \sin\tau \sin\theta\right)\sqrt{\cot^2\kappa + 1}}{\cos\tau - \sin\tau \cot\kappa \cos\theta} \quad . \tag{17}$$

6. Conclusions

The Blade Element Momentum Theory (BEMT) can be extended to an Unsteady Blade Element Momentum Theory (UBEMT). For the UBEMT the rotor disc needs to be divided not only along the radius, r but also over the blade angle, θ (Figure 10). One more calculation loop is necessary to account for the blade angle (Figure 11). An equation (17) is derived for the speed ratio, λ, which accounts for the geometry in a rotor with pronounced cone and axis angle. The UBEMT can be used to calculate unconventional geometries like the Wagner rotor. The Wagner rotor still has a slight chance to reach economic advantages as a deep sea offshore wind turbine over other configurations. Conventional horizontal axis wind turbines (HAWT) often show small cone and axis angles to reach sufficient clearance between blade and tower – especially if the rotor is located upwind from the tower and the blades are flexible and highly loaded. The accuracy of power calculations of these HAWTs can be slightly improved using the UBEMT. Although the aerodynamic coefficients used in the UBEMT are from measurements in steady flow conditions, they have been used with success in an UBEMT.

Funding: This research received no external funding.

Data Availability Statement: All relevant data is contained in the document.

Acknowledgments: Salar Ali wrote an initial draft of the manuscript based on the appendix in [12].

Conflicts of Interest: The author declared no conflict of interest.

References

1. Koh, J.H.; Ng, E.Y.K.: Downwind Offshore Wind Turbines: Opportunities, Trends and Technical Challenges. In: *Renewable and Sustainable Energy Reviews*, vol. 54 (2016), pp. 797-808. https://doi.org/10.1016/j.rser.2015.10.096.
2. Bak, C.: Aerodynamic Design of Wind Turbine Rotors. In: *Wind Energy Systems*. Woodhead Publishing Series in Energy, 2011, pp. 161-207. https://doi.org/10.1533/9780857090638.2.161
3. Brøndsted, P., Nijssen, R. P.L.: *Advances in Wind Turbine Blade Design and Materials*. Woodhead Publishing Series in Energy, 2013. ISBN 978-0-85709-426-1.
4. Zhao, D.; Han, H.; Goh, E; Cater, J.; Reinecke, A.: *Wind Turbines and Aerodynamics Energy Harvesters*. Academic Press, Elsevier, 2019. https://doi.org/10.1016/B978-0-12-817135-6.00001-6.

5. Schatter, W.: *Windkonverter: Bauarten, Wirkungsgrade, Auslegung*. Braunschweig, Germany: Vieweg, 1987.
6. Schaffarczyk. A.P.: *Einführung in die Windenergietechnik*. München, Germany, Hanser. 2022. https://doi.org/10.3139/9783446473225.
7. Kusiek, A.: *Windenergieanlagen: Technologie – Funktionsweise – Entwicklung*. München, Germany: Hanser, 2022. https://doi.org/10.3139/9783446472877
8. Hau, E.: *Windkraftanlagen: Grundlagen. Technik. Einsatz. Wirtschaftlichkeit*. Springer, 2016. https://doi.org/10.1007/978-3-662-53154-9
9. Mitschel, H.: Die Großwindanlage GROWIAN – Eine moderne Windenergieanlage in Norddeutschland. In: *Forschung in der Kraftwerkstechnik*, 1980, pp. 23-30.
10. International Standard IEC 61400-1: Wind turbines – Part 1: Design Requirements, 2005
11. Jamieson, P.: *Innovation in Wind Turbine Design*. Wiley, 2011. https://doi.org/10.1002/9781119975441.
12. Lindemann, D.: Zur aerodynamischen Berechnung eines Windenergiekonverters am Beispiel des Wagner-Rotors. Seminarvortrag. Universität Hannover, Institut für Mechanik, 1985. https://nbn-resolving.org/urn:nbn:de:gbv:18302-aero1985-06-19.01.
13. Chen, J.; Wang, Q.: Wind Turbine Airfoils and Blades – Optimization Design Theory. China Science Publishing & Media, De Gruyter, 2018. https://doi.org/10.1515/9783110344387.
14. Burton, T.; Jenkins, N.; Sharpe, D.; Bossanyi, E.: *Wind Energy Handbook*, 2011. https://doi.org/10.1002/9781119992714.
15. Manwell, J.F.; McGowan, J.G.; Rogers, A. L.: *Wind Energy Explained: Theory, Design and Application*. Wiley, 2009. https://doi.org/10.1002/9781119994367.
16. Riziotis, V.A.; Madsen, H.A.: Aeroelasticity and Structural Dynamics of Wind Turbines. In: *Wind Energy Systems*. Woodhead Publishing Series in Energy, 2011, pp. 46-111. https://doi.org/10.1533/9780857090638.1.46.
17. Rekioua, D.: *Wind Power Electric Systems: Modeling, Simulation and Control*. Springer, 2014. https://doi.org/10.1007/978-1-4471-6425-8.
18. Tong, Wei.: *Wind Power Generation and Wind Turbine. Design*. Southhampton, Boston: WIT Press, 2010. https://n2t.net/ark:/13960/t56d9866g.
19. Hachim, G.M.; Mahdi, J.A.: Analytical Assessment of the Effects of Blade Cone Angle on the Aerodynamic Performance of the Horizontal Axis Wind Turbine. In: *IOP Conference Series: Materials Science and Engineering*, vol. 671 (2019). 3rd International Conference on Engineering Sciences, 4–6 November 2019, Kerbala, Iraq. https://doi.org/10.1088/1757-899X/671/1/012140.
20. Marten, D.: QBlade v0.95 – Guidelines for Lifting Line Free Vortex Wake Simulation. TU Berlin, 2016. https://doi.org/10.13140/RG.2.1.1663.1929.
21. Hansen, M.O.L.: *Aerodynamics of Wind Turbines*. Earthscan, 2008. https://perma.cc/BAW3-N5SB.
22. Lindemann, D.: Übertragbarkeit von Meßwerten aus Versuchen an Windrädern im Hinblick auf Windkanalversuche am Wagner-Rotor. Studienarbeit. Universität Hannover, Institut für Mechanik, 1985. https://nbn-resolving.org/urn:nbn:de:gbv:18302-aero1985-07-01.014.
23. Lindemann, D.: Berechnung der reibungsfreien Strömung in Rotoren von Windkraftanlagen. Diplomarbeit. Universität Hannover, Institut für Mechanik, 1988. https://nbn-resolving.org/urn:nbn:de:gbv:18302-aero1988-02-19.017.
24. Salcedo Campoamor, L.: Calculating the Power of Wind Turbines with the Blade Element Momentum Theory. Master Thesis. Hamburg University of Applied Sciences, Aircraft Design and Systems Group (AERO). Available from: https://nbn-resolving.org/urn:nbn:de:gbv:18302-aero2017-08-18.015.
25. Wagner, G.: Wagner Rotors: Clean Energy from the Sea [Ship-Based Wind Turbine]. In: *Windkraft Journal*, vol. 2, no. 3, pp. 108-110 (Sept. 1982). Abstract: https://www.osti.gov/etdeweb/biblio/5972355.
26. Wagner, G.: The Realization of an Offshore Windmill at a Cost of 500 U.S.$/kW. In: *International Symposium Wind Energy Systems, Proceedings* (Stockholm, Sweden, 21-24 Sep 1982). Cranfield, United Kingdom: British Hydromechanics Research Association, 1982, vol. 2, conference 4, pp. 465-466. Abstract: https://www.osti.gov/etdeweb/biblio/5228239.
27. Paduch, W; Richter, B; Sasse, I; Westram, A.: Measurements on the Wagner Rotor I Experimental Vessel. Hamburg, Germany: Germanischer Lloyd. Sponsor: Bonn, Germany: Bundesministerium für Forschung und Technologie (Contract 03-E-8488-A). Schiffstechnische Beratung (STB). STB Bericht 1296-85, 74 pages. Abstract: https://www.osti.gov/etdeweb/biblio/5771479. Available from: https://www.tib.eu/en/search/id/TIBKAT:017037697.
28. Marten, D.: QBlade: a Modern Tool for the Aeroelastic Simulation of Wind Turbines. Dissertation. TU Berlin, 2020. https://doi.org/10.14279/depositonce-10646.